

Research Article

Optimizing Operating Conditions for Oxidative Coupling Methane (OCM) in the Presence of NaCl-MnO_x/SiO₂

Manisa Thanasiriruk, Patcha Saychoo, Chalempol Khajonvittayakul, Vut Tongnan and Unalome Wetwatana Hartley*
Department of Chemical and Process Engineering, The Sirindhorn International Thai-German Graduate School of Engineering (TGGS), King Mongkut's University of Technology North Bangkok, Bangkok, Thailand

Navadol Laosiripojana

The joint Graduate School of Energy and Environment, King Mongkut's University of Technology Thonburi, Bangkok, Thailand

* Corresponding author. E-mail: unalome.w.cpe@tggs-bangkok.org DOI: 10.14416/j.asep.2020.10.001
Received: 26 June 2020; Revised: 17 August 2020; Accepted: 20 August 2020; Published online: 1 October 2020
© 2021 King Mongkut's University of Technology North Bangkok. All Rights Reserved.

Abstract

A novel NaCl-MnO_x/SiO₂, synthesized using slurry mixed method, was used as a catalyst in oxidative coupling of methane process. Optimal conditions were determined using both computational and experimental methods. NaCl, MnO_x and SiO₂ which are the component of our catalyst are studied. In this research, the catalyst provided the best experimental result when the ratio of MnO_x to SiO₂ was 2 to 1. CH₄ conversion, C₂₊ selectivity, C₂₊ yield and C₂H₄/C₂H₆ ratio were achieved at 38%, 71%, 27% and 7.2, respectively when operated the process at optimal temperature of 750°C under atmospheric pressure with ratio of CH₄:O₂ at 4 and 3000 mL g⁻¹ h⁻¹ of weight hourly space velocity (WHSV). The catalytic performance of NaCl-MnO_x/SiO₂, was found to be higher than other recently developed catalysts. Besides, NaCl-MnO_x/SiO₂ gave only less than 10% selectivity of the unwanted CO₂, while the other SiO₂-based catalysts reported as high as 17% of CO₂ selectivity. It also achieved high ethylene production when benchmark with previous research. The experimental results were validated using Aspen Plus at temperature ranging from 700 to 850°C.

Keywords: Oxidative coupling of methane (OCM), Ethylene production, Methane conversion, Novel catalyst

1 Introduction

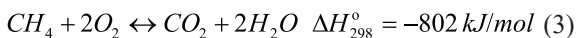
Ethylene, a well-known key building block in petrochemical industry, can be utilized to many valuable chemicals i.e. polyethylene, ethylene dichloride, ethyl benzene, and vinyl acetate which are widely usage [1]–[4]. Ethylene is conventionally produced via cracking process of natural gas/crude oil which plays a major role for productions of highly valuable products from lower value of raw materials [5], although the process is reliable on fossil fuels, high energy consumption and releases large quantity of carbon dioxide (CO₂)

[6]. Oxidative coupling of methane (OCM) is an alternative method to produce olefins from methane and oxygen. Its advantages include 1) being independent from fossil fuels as it can utilize methane from alternative resources such as shale gas, synthetic methane from methanation process or methane-rich biogas 2) flexibility in using oxygen-based greenhouse gases as oxygen source, i.e. CO₂ or N₂O, instead of pure oxygen or air, and 3) more environmentally friendly as it could release zero carbon emission [7]. OCM consists of 2 main reactions, shown as Equations (1) and (2) [7].

Please cite this article as: M. Thanasiriruk, P. Saychoo, C. Khajonvittayakul, V. Tongnan, U. W. Hartley, and N. Laosiripojana, "Optimizing operating conditions for Oxidative Coupling Methane (OCM) in the presence of NaCl-MnO_x/SiO₂," *Applied Science and Engineering Progress*, vol. 14, no. 3, pp. 477–488, Jul.–Sep. 2021, doi: 10.14416/j.asep.2020.10.001.



Oxygen concentration must be limited as it can shift the reaction towards complete combustion [Equation (3)] and partial oxidation process [Equation (4)] instead, giving CO₂ and CO as unwanted by-products, respectively [8].



Low methane conversion (~20–30%) and low ethylene selectivity (~20–30%) had been reported as the main challenge of the OCM process when using the latest developed catalyst systems such as alkali-chloride based metal oxides [9]–[11]. A promising method that can be applied to resolve the above drawbacks is the design of effective catalyst properties, including catalyst compositions and/or surface textural, together with optimizing operating conditions [12], [13]. Amongst the recently developed catalysts, manganese oxides were reported to have the highest catalytic performance towards OCM due to its high electrical conductivity [14]. For example, by using an alkali chloride-promoted manganese oxide catalysts, NaCl/Mn oxide, 25.7% ethylene yield can be produced at 750°C [10]. SiO₂ has been used as support material. Calcination condition of SiO₂ showed the effect to phase and structure of the material [15]. Amorphous silica can yield active but very unselective catalysts whereas crystalline SiO₂ can active and highly selective catalysts with respect to the formation of ethylene and Na is a promoter in term of both structural and chemical side [16]. Highly crystallite α -cristobalite SiO₂ was proven to be highly selective for ethylene production whereas Na was found to be a beneficial alkali when used as structural and chemical promoter [14]–[17]. Preparing Na₂WO₄–Mn/SiO₂ catalysts by different methods can transformed α -cristobalite into highly crystallite α -cristobalite [18]. A promising of Mn₂O₃–Na₂WO₄/SiO₂ catalyst showed the highest ethylene yield of 12.9% and ratio of ethylene and ethane at 1.3 can be achieved at 750°C, CH₄/O₂ ratio of 8 and high space velocities of 1.5x10⁵ h⁻¹ GHSV which has demonstrated these catalyst achieved at high

pressures and high space velocities too [19].

In this work, applying of NaCl–MnO_x/SiO₂ as a catalyst for OCM reaction was studied. Its catalytic performance and the role of each catalyst component towards OCM were investigated. Optimal conditions of the process and the catalyst preparation; i.e. operating temperature, weight hourly space velocity (WHSV), molar feed ratio, and ratio of SiO₂ to NaCl–MnO_x; were determined using experimental and/or computational program to achieved high ethylene production as show in C₂₊ selectivity/yield and ethylene to ethane ratio and also low CO_x production.

2 Experimental Methodology

2.1 Catalyst preparation and characterization

NaCl–MnO_x/SiO₂ was synthesized using slurry mixed route method [20]. NaCl 64% by molar (99.9%, Ajax Finechem) was dissolved in distilled water, together with Mn (NO₃)₂·4H₂O (97%, Panreac) and SiO₂ nanoparticles (98%, Ajax Finechem) at the selected ratios of MnO_x to SiO₂ of 2:1, 1:1 and 4:1. The mixed solution was added to 50 mL of a complexing agent, NH₃ solution (30%, Panreac) and allowed to stir at room temperature until the solution was homogeneous. And the solution was then heated up to 95°C. The residual was dried in a vacuum oven at 110°C overnight and pre-calcined at 400°C for 9 h. The synthesized NaCl–MnO_x/SiO₂ catalyst was crushed and then sieved to 75–180 μm. After that, it was calcined in situ at 700°C in packed-bed reactor for 2 h to obtain NaCl–MnO_x/SiO₂ powder.

2.2 Experimental set-up

A 2 g NaCl–MnO_x/SiO₂ was packed in a quartz tubular reactor (i.d.=10 mm, o.d.=13 mm, length = 50 cm). The reactor was placed in the middle of an electric furnace (Inconel, 10 cm heating zone) where the bed's temperature was measured using a K-type thermocouple. Figure 1 illustrates rig's configuration. A mixture of CH₄ (40% CH₄/Ar, BIG Company), O₂ (40% O₂/Ar, BIG Company) and Ar (99.995%, BIG Company) were fed into the system using mass flow controllers (Brooks instrument flow, 0–220 mL/min). Argon was used as a make-up gas to adjust the total volumetric flow rate. The gaseous products; CH₄,

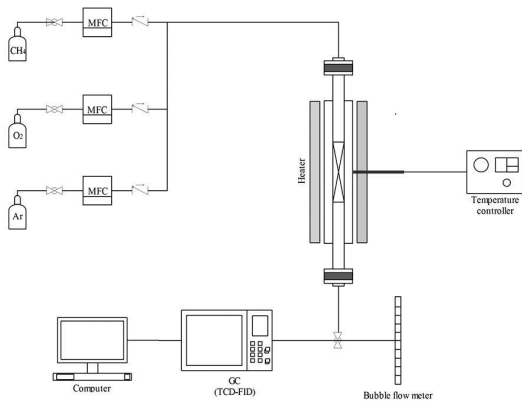


Figure 1: Schematic diagram of OCM experimental setup.

O₂, CO, CO₂, C₂H₄ and C₂H₆; were analyzed using on-line gas chromatography (Shimadzu GC-2014, FID-TCD detector) coupled with a Porapak Q capillary column.

Experimental results were demonstrated in terms of %conversion, %yield, %product selectivity which were calculated as shown in Equations (5)–(10).

$$CH_4 \text{ conversion}(\%) = \frac{\text{mole of } CH_4 \text{ consumed}}{\text{mole of } CH_4 \text{ in the feed}} \times 100\% \quad (5)$$

$$C_{2+} \text{ selectivity}(\%) = \frac{\text{mole of } C_{2+} \text{ hydrocarbon}}{\text{total mole of carbon in the product}} \times 100\% \quad (6)$$

$$CO \text{ selectivity}(\%) = \frac{\text{mole of } CO \text{ hydrocarbon}}{\text{total mole of carbon in the product}} \times 100\% \quad (7)$$

$$CO_2 \text{ selectivity}(\%) = \frac{\text{mole of } CO_2 \text{ hydrocarbon}}{\text{total mole of carbon in the product}} \times 100\% \quad (8)$$

$$C_{2+} \text{ yield}(\%) = \frac{CH_4 \text{ conversion} \times C_{2+} \text{ selectivity}}{100} \quad (9)$$

$$C_2H_4 / C_2H_6 \text{ (mol/mol)} = \frac{\text{moles of } C_2H_4}{\text{moles of } C_2H_6} \quad (10)$$

2.3 Computational analysis using Aspen plus

Equilibrium concentration of each compounds were computationally calculated at each temperature in the range of 700–850°C under atmospheric by using Aspen Plus program to validate the efficiency of

experimental results. OCM Reaction Network Presented by Stansch *et al.* were used for this simulation [21], [22]. The OCM process consists of nine heterogeneous and one homogeneous reaction steps as shown in Equations (1)–(4), (11), (16), (20), (22)–(25). An initial composition of 4 to 1 of methane/oxygen balanced with argon was used in equilibrium reactor.

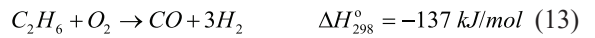
Oxidative coupling methane (OCM)



Methane partial oxidation (POM)



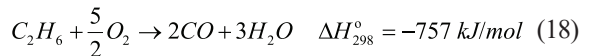
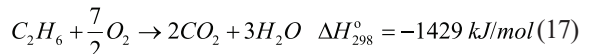
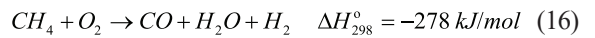
C₂ partial oxidation



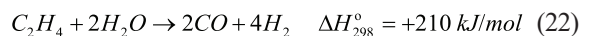
Methane combustion



Combustion hydrocarbons



Steam reforming reaction



Hydrocarbon cracking reaction



Water gas shift reaction



CO oxidation reaction



Coke formation, carbon cracking



Boudouard reaction



3 Results and Discussion

3.1 Diffractograms of NaCl-MnO_x/SiO₂

Representative samples of fresh catalyst obtained from two different calcination temperatures at 400°C and after in situ calcined at 700°C for 2 h were examined by X-ray diffraction (XRD). Figure 2(a) shows the XRD pattern obtained after 400°C calcination for 9 h of the NaCl-MnO_x/SiO₂. The material showed 1) NaCl phase structure where its diffraction peaks were presented at $2\theta = 27.33^\circ$, 45.39° , 53.82° , 56.42° , 66.17° and 75.24° . Manganese phase was found at 32.96° . Broad peak observed in the range of 20 – 25° indicating that silica oxide is amorphous phase [23]. Figure 2(b) shows the sharp peak of SiO₂ cristobalite at 21.91° and small peaks at 28.37° and 36.07° which is form after in situ calcined at 700°C for 2 h. It correspond to the formation of highly crystalline SiO₂ cristobalite due to the addition of NaCl could induce phase transformation at lower temperature [14]. Another phase of SiO₂ was observed at 20.81° , 26.6° , 36.5° , 50.08° , 59.94° and 68.06° , which corresponds to α -SiO₂. Both SiO₂ cristobalite and α -SiO₂ is highly

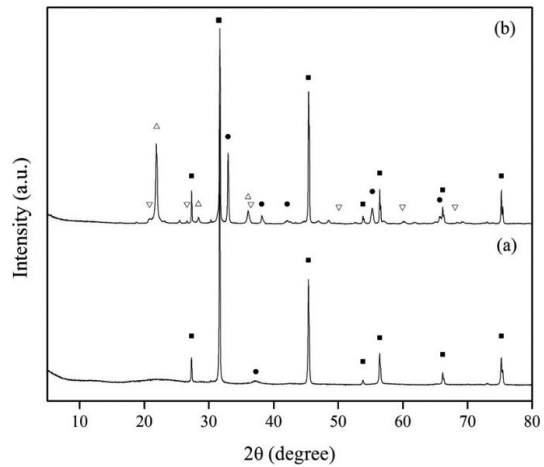


Figure 2: X-ray diffraction patterns of NaCl-MnO_x/SiO₂ (2:1) at (a) 400°C and (b) 750°C calcination temperature. The (■), (●), (▽), and (△) symbols correspond to the peaks of NaCl, Mn₇O₈SiO₄, α -SiO₂ and SiO₂ cristobalite, respectively.

selective catalysts [15], [24]. And Mn₇O₈SiO₂ was observed at 32.96° , 38.15° , 42.1° , 55.27° and 65.7° . No other additional peaks was observed, indicating that NaCl-MnO_x/SiO₂ was successfully prepared using the slurry mixed route.

3.2 Catalyst performance

3.1.1 Effect of reaction temperature

The effect of reaction temperatures was studied from 700 to 850°C on 1) CH₄ and O₂ conversion, 2) selectivity of C₂₊, CO and CO₂, and 3) yield of C₂₊. It obtained from computational results and experimental results by homogeneous reaction and heterogeneous reaction. NaCl-MnO_x/SiO₂ (64%NaCl, ratio of MnO_x:SiO₂ = 2:1) was tested at WHSV of 3000 mL/g.h and feed ratio (CH₄ to O₂) of 4 to 1. From Figure 3(a) shows CH₄ conversion and O₂ conversion as a function of temperature, the results demonstrate that near-complete conversion of O₂ can be obtained whereas 47–50% CH₄ conversion from model, 0–3% from non-catalytic and 27–38% from experiments with using NaCl-MnO_x/SiO₂ as catalyst were achieved. This indicated that O₂ was the limiting reactant which can react in many pathways, including mainly associated reactions as methane partial oxidation [Equation (12)]

and complete methane combustion [Equations (14) and (15)], were also involved in the OCM process [25]. Theoretically, no production of C_{2+} was predicted, shown in Figure 3(b) and (c) for the results obtained from computer simulation. CO formation was expected at 100% selectivity, indicating that the overall OCM reaction mainly occurred via methane partial oxidation pathway in theory. Small amount of CO_2 formation, at low temperature lower than $700^\circ C$, was also suggested by the computational analysis. This result is corresponding to non-catalytic reaction but CO_2 formation was not detected.

However, the experimental results with using $NaCl-MnO_x/SiO_2$ shown in Figure 3(b) and (c) showed the opposite result, as C_{2+} production was observed at all temperatures. The maximum productivity was obtained at $750^\circ C$ where yield and selectivity of C_{2+} were reported at 23% and 61%, respectively. CO selectivity was increased when the temperature increased due to its endothermicity ($\Delta H = +210 \text{ kJ/mol}$) [Equation (22)] [26]. CO_2 selectivity was the highest at $700^\circ C$ as it was a by-product of full combustion ($\Delta H = -802 \text{ kJ/mol}$) [Equation (14)] [24], [27], which is well-known to occur at temperature ranging from 450 up to $1000^\circ C$ [27]–[29]. The OCM process was then concluded to be a highly selective reaction and unlikely to occur without a catalyst [30]. From the experimental results, C_{2+} production was encouraged by $NaCl-MnO_x/SiO_2$ catalyst due to its effective alkali and transition metals. $NaCl$ offered great performance on the selective formation of ethylene and also suppressed CO formation [11], [31]–[34]. C_{2+} productivity was increased when the temperature increased from 700 to $750^\circ C$, although decreased when the temperatures were higher than $750^\circ C$ because of an involvement of C_{2+} cracking/steam reforming, and also the deactivation of catalyst in such temperature range [35]–[37]. At this temperature range, the steam reforming [Equation (21)], reverse water gas shift [Equation (25)], and combustion of hydrocarbons [Equations (16)–(20)] led to the rise in CO and CO_2 formation and were also involved as reported earlier in many previous works [36]–[38]. Carbon cracking [Equations (27)–(30)] occurred coke accumulation and affect catalyst deactivation [36]. In addition, thermal deactivation of the catalyst is occurred from melting of sodium chloride (the melting point of sodium chloride is approximately $800^\circ C$) which is very important factor

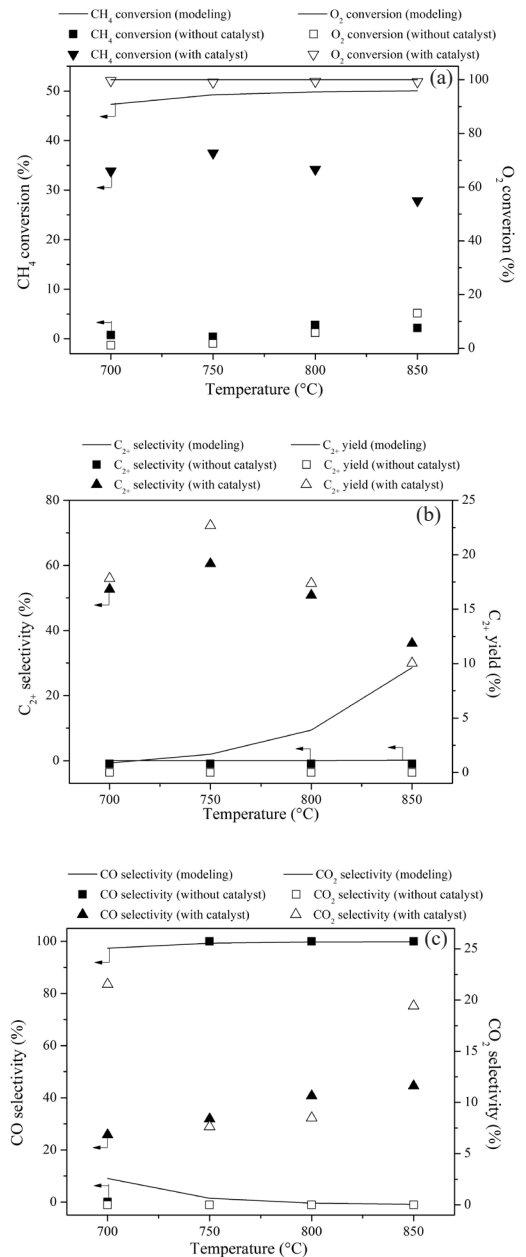


Figure 3: Comparison of results between reaction's activities achieved a) methane conversion and oxygen conversion b) C_{2+} selectivity and C_{2+} yield and c) CO selectivity and CO_2 selectivity via model and experiment (without catalyst and with catalyst ratio of $NaCl-MnO_x:SiO_2 = 2:1$) under WHSV of 3000 mL/g.h and feed ratio (CH_4 to O_2) of 4 to 1 in the reaction temperature range from 700 to $850^\circ C$.

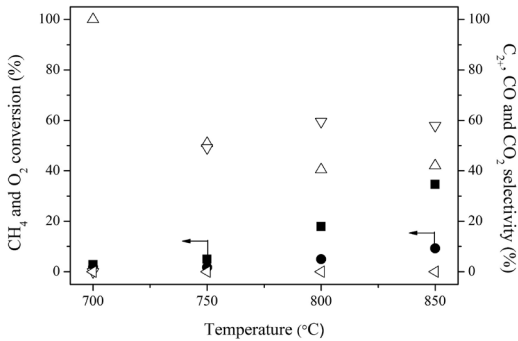


Figure 4: The effect of NaCl to CH₄ conversion (●), O₂ conversion (■), C₂₊ selectivity (△), CO selectivity (▽), and CO₂ selectivity (◁) at WHSV of 3000 mL/g.hr and feed ratio (CH₄ to O₂) of 4 to 1 in the reaction temperature range from 700 to 850°C.

for C₂₊ productivity [39]. The loss of NaCl is started to melting, water vapor reacted with sodium chloride to form hydrogen chloride and sodium hydroxide in the product stream [40]. The operating temperature lower than 800°C is therefore suitable for the use of NaCl-MnO_x/SiO₂ in OCM process.

3.1.2 The role of NaCl, MnO_x, and SiO₂ in the NaCl-MnO_x/SiO₂ on catalytic performance

NaCl, MnO_x, and SiO₂ in the NaCl-MnO_x/SiO₂ was investigated as a function of temperature ranging from 700–850°C at WHSV of 3000 mL/g.h and feed ratio (CH₄ to O₂) of 4 to 1 in terms of 1) CH₄ and O₂ conversion and 2) selectivity of C₂₊, CO and CO₂.

Figure 4 shows the results of NaCl performance. It demonstrates that NaCl affected to both CH₄ conversion, which increased from 1.75% at 700°C to 9.25% at 850°C, and O₂ conversion, which increased from 2.80% at 700°C to 34.64% at 850°C. However, C₂₊ selectivity decreased when temperature was raised due to C₂₊ cracking and partial oxidation reaction [Equations (15), (26), (31)] [35], [36]. And also CO selectivity increased with increasing temperature due to partial oxidation of methane and C₂₊ reaction [Equations (12) and (13)]. CO₂ was not detected at all temperatures indicated that full combustion reaction was not occurred. Therefore, NaCl is suggested to play an important role as active site for C₂₊ productivity [33]. Meanwhile, it inhibited the CO₂ formation, which is in agreement with other researchers [11], [39]–[41].

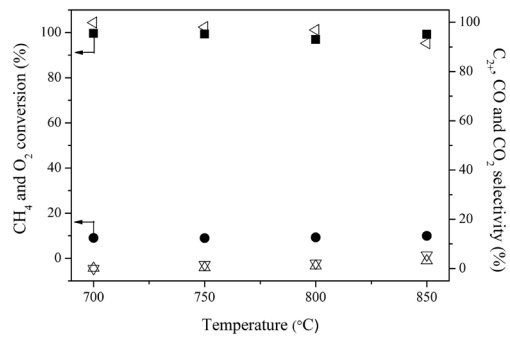


Figure 5: The effect of MnO_x to CH₄ conversion (●), O₂ conversion (■), C₂₊ selectivity (△), CO selectivity (▽), and CO₂ selectivity (◁) at WHSV of 3000 mL/g.h and feed ratio (CH₄ to O₂) of 4 to 1 in the reaction temperature range from 700 to 850°C.

MnO_x catalyst showed complete conversion of O₂, while the conversion of CH₄ was approximately at 10% all reaction temperatures studied in this work as shown in Figure 5. MnO_x could adsorb oxygen on the surface of catalyst to be surface-active oxygen by transferring electron from the surface of catalyst to oxygen molecule due to good electrical conductivity property and low energy gap [14], [42]. Mostly methane reacted with surface-active oxygen via complete methane combustion, evidenced by high CO₂ production for all temperatures. At high temperature, CO₂ formation slightly decreased due to an increase of CO selectivity by Boudouard reaction [Equation (31)] [43], [44]. Moreover, increasing of CO selectivity occurred partial oxidation of methane. Therefore, MnO_x provided large amount of surface-active oxygen which represents an increasing of the surface lattice oxygen mobility is increased but it affected to lower C₂₊ production [14], [34].

Figure 6 showed the results of SiO₂ support catalyst for the OCM. Maximum O₂ conversion (99.6%) and CH₄ conversion (15%) were occurred at the highest temperature. The difference between the results of SiO₂ and homogeneous reaction demonstrated that SiO₂ affect C₂₊ formation due to the OCM pathway [45]. Methane partial oxidation occurred which can be seen from almost 100% CO selectivity at 700°C. Decreasing of CO caused by the reduction of methane concentration due to methane cracking over than 700°C [46]. It demonstrates that the ratio of methane to oxygen decreased to occur complete methane combustion as seen from the increase of carbon dioxide selectivity,

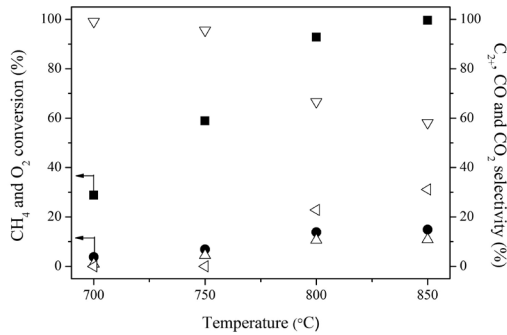


Figure 6: The effect of SiO₂ to CH₄ conversion (●), O₂ conversion (■), C₂₊ selectivity (△), CO selectivity (▲), and CO₂ selectivity (▼) at WHSV of 3000 mL/g.hr and feed ratio (CH₄ to O₂) of 4 to 1 in the reaction temperature range from 700 to 850°C.

oxygen conversion and methane conversion. Thereby, SiO₂ based catalyst is considered to play a vital role for C₂₊ productivity and the consumption of methane and oxygen.

3.1.3 Effect of Weight hourly space velocity (WHSV)

2 grams of NaCl-MnO_x/SiO₂ was used in the following experiments by vary total inlet flow rates, all carried out at 750°C. Ratio of CH₄ to O₂ was fixed at 4. The effect of WHSV was varied in range 1500–6000 mL/g.h at 1500, 2250, 3000, 3750, 4500, and 6000 mL/g.h. The experiments were carried out at fixed reaction temperature of 750°C and mole ratio of CH₄ to O₂ at 4.

Figure 7 presents the influence of WHSV on CH₄ conversion, C₂₊ and CO_x selectivity, C₂ yield and C₂H₄/C₂H₆ mole ratio. At 6000 mL g⁻¹ h⁻¹, it was found that methane conversion and C₂₊ product were low due to short contact time. Mostly methane flowed through catalyst without reacting but some part of methane was consumed, resulted in undesired product CO_x. Increasing of residence time caused an increase of methane conversion and C₂₊ selectivity but lower CO_x selectivity. It was supported one of the assumption that CO_x formation depends on the residence time of reaction. The homogeneous reaction in the gas phase might occur when the residence time in the catalyst bed is too short [25]. Ratio of ethylene to ethane increased with decreasing of WHSV indicated that ethylene formation occurred via continually reaction. At a longer residence time (low WHSV), the remaining

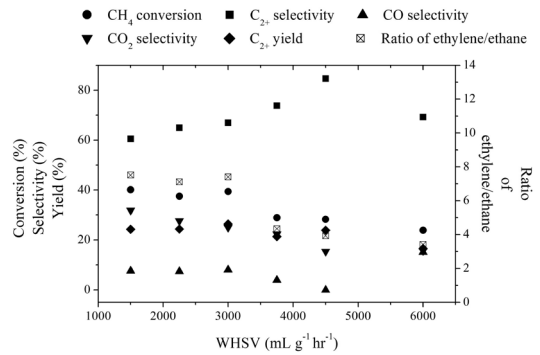


Figure 7: Methane conversion (●), C₂₊ selectivity (■), CO selectivity (▲), CO₂ selectivity (▼), C₂₊ yield (◆) and C₂H₄/C₂H₆ ratio (⊠) with catalyst ratio of NaCl-MnO_x:SiO₂ = 2:1 under different WHSV with a reaction temperature at 750°C in ratio of methane and oxygen is 4.

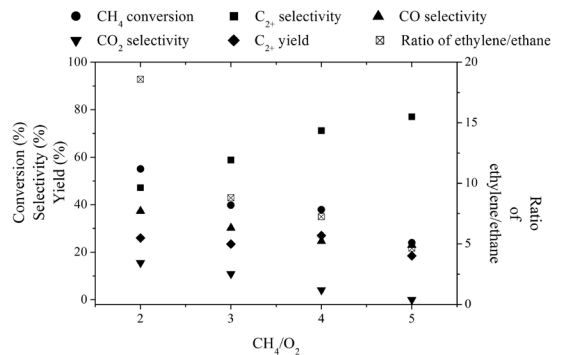


Figure 8: Methane conversion (●), C₂₊ selectivity (■), CO selectivity (▲), CO₂ selectivity (▼), C₂₊ yield (◆) and C₂H₄/C₂H₆ ratio (⊠) with catalyst ratio of NaCl-MnO_x:SiO₂ = 2:1 under different inlet molar ratio of methane and oxygen with a reaction temperature at 750°C in WHSV of 3000 mL g⁻¹ h⁻¹.

oxygen in the reactor formed nonselective products as CO_x. It demonstrated that ethylene and ethane are an intermediate components [15], [37], [47]. The best performance was observed that C₂₊ yield (27%) and molar ratio of C₂H₄/C₂H₆ (7.2) obtained when the WHSV was at 3000 mL g⁻¹ h⁻¹.

3.1.4 Effect of feed ratio

The effect of CH₄ to O₂ feed ratio was studied in the range from 2 to 5 at reaction temperature of 750°C. Figure 8 showed the effect of the feed ratio on catalytic

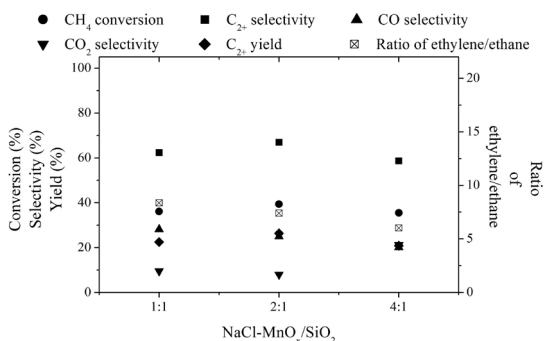


Figure 9: Methane conversion (●), C₂₊ selectivity (■), CO selectivity (▲), CO₂ selectivity (▼), C₂₊ yield (◆) and C₂H₄/C₂H₆ ratio (⊠) under different NaCl-MnO_x:SiO₂ ratio in 3000 mL/g.hr WHSV and CH₄/O₂ ratio is 4 at 750°C of reaction temperature.

performance of the NaCl-MnO_x/SiO₂ towards OCM reaction. CH₄ conversion was observed to decrease with increasing ratio of methane and oxygen whereas the C₂₊ selectivity increased when CH₄/O₂ ratio was increased. CO and CO₂ selectivity decreases with increasing CH₄/O₂ ratio, which affects oxidation of CO, and CO₂. This result is in good agreement with the work reported by Farrell *et al.* [21], of which reported the decrease of CH₄/O₂ molar ratio led to an increase of CO and CO₂ production. When the methane was fed excess, the reaction pathway is likely toward the production of C₂. Appropriate ratio of methane to oxygen for achieved 25% C₂₊ yield is at 4.

3.1.5 Effect of NaCl-MnO_x to SiO₂ molar ratio

The amount of active site NaCl-MnO_x was investigated for the effect to OCM process performance was investigated by varying NaCl-MnO_x to SiO₂ mole ratio at 1:1, 1:2, and 1:4.

The results in Figure 9 demonstrated that the amount of active site affect process performance. It has been seen that the activity of catalyst and product selectivity were increased when increasing of NaCl-MnO_x (active site) and it also caused CO_x is decreased. It was following the OCM mechanisms that oxygen adsorption on the catalyst surface. Hydrogen abstraction from methane occur on the catalyst surface to form methyl radicals. Ethane formation was occurred from couple methyl radicals.

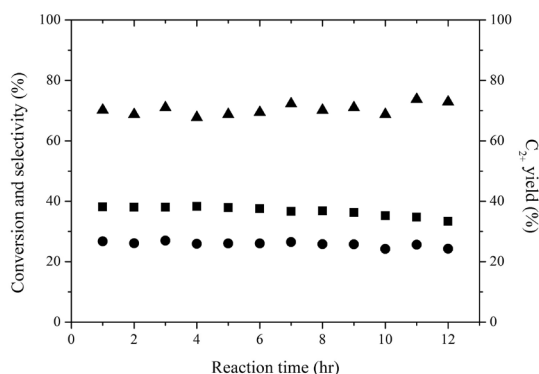


Figure 10: Methane conversion (■), C₂₊ selectivity (▲), and C₂₊ yield (●) with catalyst ratio of NaCl-MnO_x:SiO₂ = 2:1 in 3000 mL/g.h WHSV and CH₄/O₂ ratio is 4 at 750°C of reaction temperature.

Then dehydrogenation reaction was occurred to form ethylene [22], [26], [48]. At active site to support ratio of 4, methane conversion and C₂₊ selectivity were decreased due to less area of support that make poor distribution of the active site and also the unification of active site without support decreased the surface reaction causing C₂₊ yield to decreased [45]. At 2:1 of NaCl-MnO_x to SiO₂ achieved the methane conversion, C₂₊ selectivity and C₂₊ yield at 750°C about 39, 66 and 26%, respectively.

3.1.6 Catalyst stability

Figure 10 shows NaCl-MnO_x/SiO₂ catalyst was stable throughout a 12 h run at 750°C, 3000 mL/g.h WHSV and CH₄/O₂ ratio is 4.

The CH₄ conversion was stabilized at about 38 ± 3.4% and the best C₂₊ selectivity reached 72 ± 1.6%. C₂₊ yield maintained at 27 ± 1.2% during 12 h period continuous reaction without recharging the catalyst. The optimum condition can stabilized the performance of NaCl-MnO_x/SiO₂.

Table 1 was summarized performances of the process for different catalysts in terms of reactant conversion and product selectivity under OCM reaction. NaCl-MnO_x/SiO₂ developed in our work shows superior catalytic properties as it could be operated at low temperature to achieve high performance as C₂₊ yield, and ethylene to ethane about 7.2 at optimum conditions.

Table 1: Catalytic performance for oxidative coupling of methane over various catalysts

Catalyst	Operating Condition	CH ₄ Conversion	C ₂₊ Yield	C ₂₊ Selectivity	C ₂ H ₄ /C ₂ H ₆	Ref.
Na-CaO	T = 750°C, CH ₄ /O ₂ = 4	24.7	17	68.8	1.2	[47]
K-CaO	WHSV = 5140 cm ³ ·g ⁻¹ ·h ⁻¹	25.2	14.8	58.9	1.2	
Mn/Na ₂ WO ₄ /SiO ₂	T = 775°C, CH ₄ /air = 7.5	20	16	80	1.4	[14]
Li-TbO _x /n-MgO	T = 700°C CH ₄ /O ₂ = 4	24.9	14.5	63.6	1.4	[49]
Li-Sm ₂ O ₃ /n-MgO	GHSV = 2400 h ⁻¹	24.4	13.2	62.5	1.7	
Ce-Mn-Na ₂ WO ₄ /SiO ₂	T = 800°C, CH ₄ /air = 1	21	-	84	-	[48]
Mn-Na ₂ WO ₄ /SiO ₂	T = 800°C, CH ₄ /air = 2	45.4	19.5	41.4	-	[50]
Mn-Na ₂ WO ₄ /SiO ₂	T = 825°C, CH ₄ /O ₂ = 2.5	35.4	20.6	58.1	2.75	[51]
Mn-Na ₂ WO ₄ /n-SiO ₂	T = 800°C, CH ₄ /O ₂ = 4	25.2	18.5	73.3	1.7	[24]
MnxOy-Na ₂ WO ₄ /SiO ₂ -rutile	T = 750°C, CH ₄ /O ₂ = 4	6.5	3.5	58.6	-	[52]
MnxOy-Na ₂ WO ₄ /SBA-15	T = 750°C	13	-	68	-	[53]
NaCl-MnO _x /SiO ₂	T = 750°C CH ₄ /O ₂ = 4 WHSV = 3000 cm ³ ·g ⁻¹ ·h ⁻¹	38	27	71.2	7.24	Our work

4 Conclusions

The developed NaCl-MnO_x/SiO₂ catalyst, which was synthesized by using slurry mixed method, showed a good performance for OCM reaction as thermodynamic limitation could be overcome. C₂₊ selectivity could be increased by NaCl and SiO₂ whereas MnO_x and SiO₂ improved conversion of methane and oxygen. Key process parameters, including reaction temperature, WHSV, CH₄ to O₂ feed ratio, NaCl-MnO_x to SiO₂ molar ratio, were investigated. Increasing reaction temperature to lower than 800°C was found to render methane conversion, C₂₊ selectivity and ethylene and ethane ratio. The increment of WHSV, which represents low residence time in the reactor, was found to decrease methane conversion, C₂₊ yield and ratio of ethylene to ethane. An increase of methane/oxygen ratio led to lower conversion because the demand of methane in the reaction consumed less than the amount of inlet methane. The increase of active site to support ratio offered good catalytic activity; however, an excess of active site could cause active site to aggregate. Our investigation suggested that the NaCl-MnO_x/SiO₂ catalyst exhibits excellent and stability performance for the OCM reaction. High methane conversion, C₂₊ selectivity, C₂₊ yield and C₂H₄/C₂H₆ ratio about 38%, 71%, 27% and 7.2, respectively, could be obtained with using NaCl-MnO_x/SiO₂ catalyst, which was calcined at 400°C, WHSV at 3000 mL g⁻¹ h⁻¹, the

ratio of methane/oxygen at 4, active site/support of catalyst at 2 and operating temperature at 750°C. These experiment is the highest value reported so far to the best of our knowledge.

Acknowledgments

This study was supported by Department of Chemical and Process Engineering, The Sirindhorn International Thai-German Graduate School of Engineering (TGGs), King Mongkut's University of Technology North Bangkok, Bangkok (KMUTNB) and KMUTNB fund (KMUTNB-GEN-59-65).

References

- [1] S. Lewandowski, "Ethylene – Global IHS market" presented at the Asia Conference, Singapore, Nov. 2, 2016.
- [2] H. Zimmermann and R. Walzl, "Ethylene," in *Ullmann's encyclopedia of industrial chemistry*, 2012, vol. 3, pp. 465–526.
- [3] O. Adekomaya, T. Jamiru, E. Sadiku, and A. Adediran, "Sustainability of high temperature polymeric materials for electronic packaging applications," *International Journal of Applied Science and Technology*, vol. 11, no. 13, pp. 217–224, 2018.
- [4] Y. Samphawamontri, T. Srinophakun, P. Dittanet

- and K. Choroencham, “Heat integrated process design, simulation and control of polymerization and drying sections for HDPE production,” *International Journal of Applied Science and Technology*, vol. 9, no. 2, pp. 121–136, 2016.
- [5] K. Wagialla, “Petrochemical aromatics from liquid hydrocarbons a technoeconomic assesment,” presented at the 7th Saudi Engineering Conference, Riyadh, Saudi Arabia Stuttgart, Dec. 2–5, 2007.
- [6] T. Ren, M. Patel, and K. Blok, “Olefins from conventional and heavy feedstocks: Energy use in steam cracking and alternative processes,” *Energy Journal*, vol. 31, pp. 425–451, Jun. 2006.
- [7] A. Galadima and O. Muraza, “Revisiting the oxidative coupling of methane to ethylene in the golden period of shale gas: A review,” *Journal of Industrial and Engineering Chemistry*, vol. 37, pp. 1–13, Mar. 2016.
- [8] J. Kim, L. H. Park, J. M. Ha, and E. D. Park, “Oxidative coupling of methane over $\text{Mn}_2\text{O}_3\text{-Na}_2\text{WO}_4/\text{SiC}$ catalyst,” *Catalysts*, vol. 9, Apr. 2019.
- [9] C. T. Au, K. D. Chen, H. X. Dai, Y. W. Liu, J. Z. Luo, and C. F. Ng, “Oxidative dehydrogenation of ethane to ethene over BaO- and $\text{BaBr}_2\text{-}$ Modified HO_2O_3 catalysts,” *Journal of Catalysis*, vol. 179, pp. 300–308, Jul. 1998.
- [10] K. Otsuka and T. Komatsu, “Active catalysts in oxidative coupling of methane,” *Journal of the Chemical Society, Chemical Communications*, vol. 5, pp. 388–389, Jan. 1987.
- [11] K. Otsuka, Q. Liu, M. Hatano, and A. Morikawa “Synthesis of ethylene by partial oxidation of methane over the oxides of transition elements with LiCl ,” *Chemistry Letters*, vol. 15, no. 6, pp. 903–906, 1986.
- [12] J. S. Ahari, M. T. Sadeghi, and S. Z. Pashne, “Optimization of OCM reaction conditions over Na-W-Mn/SiO_2 catalyst at elevated pressure,” *Journal of the Taiwan Institute of Chemical Engineers*, vol. 42, pp. 751–759, Feb. 2011.
- [13] T. P. Tiemersma, M. J. Tuinier, F. Gallucci, J. A. M. Kuipers, and M. van Sint Annaland, “A kinetics study for the oxidative coupling of methane on a $\text{Mn/Na}_2\text{WO}_4/\text{SiO}_2$ catalyst,” *Applied Catalysis A: General*, vol. 433–434, pp. 96–108, May. 2012.
- [14] A. Malekzadeh, A. Khodadadi, M. Abedini, M. Amini, A. Bahramian, and A. K. Dalai, “Correlation of electrical properties and performance of OCM $\text{MO}_x/\text{Na}_2\text{WO}_4/\text{SiO}_2$ catalysts,” *Catalysis Communications*, vol. 2, pp. 241–247, Jul. 2001.
- [15] S. Arndt, T. Otremba, U. Simon, M. Yildiz, H. Schubert, and R. Schomäcker, “ $\text{Mn-Na}_2\text{WO}_4/\text{SiO}_2$ as catalyst for the oxidative coupling of methane. What is really known?,” *Applied Catalysis A: General*, vol. 425–426, pp. 53–61, Feb. 2012.
- [16] A. Palermo, J. P. H. Vazquez, A. F. Lee, M. S. Tikhov, and R. M. Lambert, “Critical influence of the amorphous silica-to-cristobalite phase transition on the performance of $\text{Mn/Na}_2\text{WO}_4/\text{SiO}_2$ catalysts for the oxidative coupling of methane,” *Journal of Catalysis*, vol. 177, pp. 259–266, Apr. 1998.
- [17] N. S. Hayek, N. S. Lucas, C. W. Damouny, and O. M. Gazit, “Critical surface parameters for the oxidative coupling of methane over the Mn-Na-W/SiO_2 Catalyst,” *ACS Applied Materials and Interfaces*, vol. 9, pp. 40404–40411, 2017.
- [18] J. Wang, L. Chou, B. Zhang, H. Song, J. Zhao, J. Yang, and S. Li, “Comparative study on oxidation of methane to ethane and ethylene over $\text{Na}_2\text{WO}_4\text{-Mn/SiO}_2$ catalysts prepared by different methods,” *Journal of Molecular Catalysis A: Chemical*, vol. 245, pp. 272–277, Sep. 2005.
- [19] L. Chou, Y. Cai, B. Zhang, J. Niu, S. Ji, and S. Li, “Oxidative coupling of methane over Na-W-Mn/SiO_2 catalysts at elevated pressures,” *Journal of Natural Gas Chemistry*, vol. 11, pp. 131–136, Dec. 2002.
- [20] A. Aseem and M. P. Harold, “ C_2 yield enhancement during oxidative coupling of methane in a nonpermeable porous membrane reactor,” *Chemical Engineering Science*, vol. 175, pp. 199–207, Sep. 2017.
- [21] B. L. Farrell, V. O. Igenegbai, and S. Lincic, “A viewpoint on direct methane conversion to ethane and ethylene using oxidative coupling on solid catalysts,” *ACS Catalysis*, vol. 6, pp. 4340–4346, May. 2016.
- [22] A. Farsi, A. Moradi, S. Ghader, V. Shadravan, and Z. A. Manan, “Kinetics investigation of direct natural gas conversion by oxidative coupling of methane,” *Journal of Natural Gas Science and Engineering*, vol. 2, pp. 270–274, Sep. 2010.
- [23] I. M. Alibe, K. A. Matori, E. Saion, A. M. Alibe, M. H. M. Zaid, and E. A. A. G. Engku, “A facile

- synthesis of amorphous silica nanoparticles by simple thermal treatment route,” *Digest Journal of Nanomaterials and Biostructures*, vol. 11, no. 4, pp. 1155–1164, 2016.
- [24] T. W. Elkins and H. E. Hagelin-Weaver, “Characterization of Mn-Na₂WO₄/SiO₂ and Mn-Na₂WO₄/MgO catalysts for the oxidative coupling of methane,” *Applied Catalysis A: General*, vol. 497, pp. 96–106, Feb. 2015.
- [25] S. Li, “Reaction chemistry of W-Mn/SiO₂ catalyst for the oxidative coupling of methane,” *Journal of Natural Gas Chemistry*, vol. 12, pp. 1–9, 2003.
- [26] C. Karakaya, H. Zhua, C. Loebick, J. G. Weissman, and R. J. Kee, “A detailed reaction mechanism for oxidative coupling of methane over Mn/Na₂WO₄/SiO₂ catalyst for non-isothermal conditions,” *Catalysis Today*, vol. 312, pp. 10–22, Aug. 2018.
- [27] Z. Yang, P. Yang, L. Zhang, M. Guo, and Y. Yan, “Investigation of low concentration methane combustion in a fluidized bed with Pd/Al₂O₃ as catalytic particles,” *RSC Advances*, vol. 4, pp. 59418–59426, Oct. 2014.
- [28] C. Khajonvittayakul, V. Tongnan, T. Kangsadan, N. Laosiripojana, S. Jindasuwan, and U. W. Hartley, “Thermodynamic and mechanism study of syngas production via integration of nitrous oxide decomposition and methane partial oxidation in the presence of 10%NiO–La_{0.3}Sr_{0.7}Co_{0.7}Fe_{0.3}O_{3-δ},” *Reaction Kinetics, Mechanisms and Catalysis*, vol. 127, pp. 839–855, Jun. 2019.
- [29] J. H. Burgoyne and H. Hirsch, “The combustion of methane at high temperatures,” in *Proceedings of the Royal Society A: Mathematical, Physical*, 1954, pp. 73–93.
- [30] G. E. Keller and M. M. Bhasin, “Synthesis of ethylene via oxidative coupling of methane,” *Journal of Catalysis*, vol. 73, pp. 9–19, Aug. 1981.
- [31] I. Matsuura, Y. Utsumi, M. Nakai, and T. Doi, “Oxidative coupling of methane over lithium-promoted zinc oxide catalyst,” *Chemistry Letters*, vol. 11, pp. 1981–1984, 1986.
- [32] I. Pasquon, “New processes and perspectives in the field of heterogeneous oxidation catalysis in relation to other methods of oxidation,” *Catalysis Today*, vol. 1, pp. 297–333, 1987.
- [33] K. Otsuka, M. Hatano, and T. Komatsu, “Synthesis of C₂H₄ by partial oxidation of CH₄ over transition metal oxides with alkali-chlorides,” *Studies in Surface Science and Catalysis*, vol. 36, pp. 383–387, 1988.
- [34] R. Burch, G. D. Squire, and S. C. Tsang, “Comparative study of catalysts for the oxidative coupling of methane,” *Applied Catalysis*, vol. 43, pp. 105–116, Apr. 1988.
- [35] M. Huff, P. M. Torniainen, D. A. Hickman, and L. D. Schmidt, “Partial oxidation of CH₄, C₂H₆ and C₃H₈ on monoliths at short contact times,” *Studies in Surface Science and Catalysis*, vol. 81, pp. 315–320, 1994.
- [36] V. Fleischer, R. Steuer, S. Parishan, and R. Schomäcker, “Investigation of the surface reaction network of the oxidative coupling of methane over Na₂WO₄/Mn/SiO₂ catalyst by temperature programmed and dynamic experiments,” *Journal of Catalysis*, vol. 341, pp. 91–103, Jul. 2016.
- [37] S. M. K. Shahri and S. M. Alavi, “Kinetic studies of the oxidative coupling of methane over the Mn/Na₂WO₄/SiO₂ catalyst,” *Journal of Natural Gas Chemistry*, vol. 18, pp. 25–34, Nov. 2008.
- [38] S. Sengodan, R. Lan, J. Humphreys, D. Du, W. Xu, H. Wang, and S. Tao, “Advances in reforming and partial oxidation of hydrocarbons for hydrogen production and fuel cell applications,” *Renewable and Sustainable Energy Reviews*, vol. 82, pp. 761–780, Feb. 2018.
- [39] N. Hiyoshi and T. Ikeda, “Oxidative coupling of methane over alkali chloride–Mn–Na₂WO₄/SiO₂ catalysts: Promoting effect of molten alkali chloride,” *Fuel Processing Technology*, vol. 133, pp. 29–34, May 2015.
- [40] A. Machocki and R. Jezior, “Oxidative coupling of methane over a sodium-calcium oxide catalyst modified with chloride ions” *Chemical Engineering Journal*, vol. 137, pp. 643–652, Apr. 2008.
- [41] R. Burch, G. D. Squire, and S. C. Tsang, “Role of chlorine in improving selectivity in the oxidative coupling of methane to ethylene,” *Applied Catalysis*, vol. 46, pp. 69–87, Jan. 1989.
- [42] A. Malekzadeh, A. K. Dalai, A. Khodadadi, and Y. Mortazavi, “Structural features of Na₂WO₄–MO_x/SiO₂ catalysts in oxidative coupling of methane reaction,” *Catalysis Communications*, vol. 9, pp. 960–965, Mar. 2008.



- [43] G. D. Souza, N. M. Balzaretti, N. R. Marcilio, and O. Perez-Lopez, “Decomposition of ethanol over Ni-Al catalysts: *Effect of copper addition*,” *Procedia Engineering*, vol. 42, pp. 370–382, 2012.
- [44] A. Gupta and S. Kerdsuwan, “Efficient energy conversion of wastes and fuels in power systems,” *KMUTNB: International Journal of Applied Science and Technology*, vol. 7, no. 2, pp. 1–26, 2014.
- [45] M. R. Lee, M. J. Park, W. Jeon, J. W. Choi, Y. W. Suh, and D. J. Suh, “A kinetic model for the oxidative coupling of methane over $\text{Na}_2\text{WO}_4/\text{Mn}/\text{SiO}_2$,” *Fuel Processing Technology*, vol. 96, pp. 175–182, Apr. 2012.
- [46] X. Li, G. Zhang, K. Tang, O. Ostrovski, and R. Tronstad, “Carbothermal reduction of quartz in methane-hydrogen-argon gas mixture,” *Metallurgical and Materials Transactions B*, vol. 46, no. 5, pp. 2384–2393, 2015.
- [47] V. H. Rane, S. T. Chaudhari, and V. R. Choudhary, “Influence of alkali metal doping on surface properties and catalytic activity/selectivity of CaO catalysts in oxidative coupling of methane,” *Journal of Natural Gas Chemistry*, vol. 17, pp. 313–320, Dec. 2008.
- [48] W. Liang, S. Sarsani, D. West, A. Mamedov, I. Lengyel, H. Perez, and J. Lowrey, “Performance improvement for a fixed-bed reactor with layered loading catalysts of different catalytic properties for oxidative coupling of methane,” *Catalysis Today*, vol. 299, pp. 60–66, Jan. 2018.
- [49] T. W. Elkins, S. J. Roberts, and H. E. Hagelin-Weaver, “Effects of alkali and alkaline-earth metal dopants on magnesium oxide supported rare-earth oxide catalysts in the oxidative coupling of methane,” *Applied Catalysis A: General*, vol. 528, pp. 175–190, Nov. 2016.
- [50] S. Gua, H. S. Oh, J. W. Choi, D. J. Suh, J. Jae, J. Choi, and J. M. Ha, “Effects of metal or metal oxide additives on oxidative coupling of methane using $\text{Na}_2\text{WO}_4/\text{SiO}_2$ catalysts: Reducibility of metal additives to manipulate the catalytic activity,” *Applied Catalysis A: General*, vol. 562, pp. 114–119, Jul. 2018.
- [51] H. Godinia, A. Gili, O. Görke, S. Arndt, U. Simon, A. Thomas, R. Schomäcker, and G. Wozny, “Sol-gel method for synthesis of $\text{Mn}-\text{Na}_2\text{WO}_4/\text{SiO}_2$ catalyst for methane oxidative coupling,” *Catalysis Today*, vol. 236, pp. 12–22, Nov. 2014.
- [52] M. Yildiza, U. Simon, T. Otremba, Y. Aksu, K. Kailasam, and A. Thomas, “Support material variation for the $\text{Mn}_x\text{O}_y-\text{Na}_2\text{WO}_4/\text{SiO}_2$ catalyst,” *Catalysis Today*, vol. 228, pp. 5–14, Jun. 2014.
- [53] M. Yildiz, Y. Aksu, U. Simon, K. Kailasam, O. Goerke, F. Rosowski, R. Schomacker, A. Thomas, and S. Arndt, “Enhanced catalytic performance of $\text{Mn}_x\text{O}_y-\text{Na}_2\text{WO}_4/\text{SiO}_2$ for the oxidative coupling of methane using an ordered mesoporous silica support,” *Chemical Communications*, vol. 50, pp. 14440–14442, 2014.